Effect of PgTPhPBr on the electrochemical and corrosion behaviour of 304 stainless steel in H_2SO_4 solution

A.A. HERMAS, M.S. MORAD and M.H. WAHDAN*
Chemistry Department, Faculty of Science, Assiut University, Assiut 71516, Egypt
(*author for correspondence)

Abstract

Weight-loss, potentiodynamic polarization and electrochemical impedance spectroscopy (EIS) measurements were used to study the inhibition of 304 stainless steel corrosion in 1 M H_2SO_4 at 50 °C by propargyltriphenylphosphonium bromide (PgTPhPBr). The inhibiting effects of propyltriphenylphosphonium bromide (PrTPhPBr) and propargyl alcohol (PA) were also studied for the sake of comparison. For the investigated compounds, Tafel extrapolation in the cathodic region gave a corrosion inhibition efficiency of 98% at 1×10^{-3} M. Adsorption of both PgTPhPBr and PA was found to follow Frumkin's isotherm while adsorption of PrTPhPBr obeys that of Temkin. In the anodic domain, PgTPhPBr acted as a good passivator. The impedance spectra recorded at the corrosion potential (E_{cor}) revealed that the charge transfer process in the inhibited and uninhibited states controls corrosion of 304 stainless steel.

List of symbols

(CR)	corrosion rate (mdd)
E_{cor}	open-circuit corrosion potential (mV)
I_{cor}	corrosion current density (μA cm^{-2})
C	molar concentration of the inhibitor
E_{pp}	primary passivation potential (mV)
I_{a1}	critical current density (μA cm^{-2})
I_{a2}	second anodic current peak (μA cm^{-2})
R_{ct}	resistance of charge transfer (Ω cm^2)
R_a	resistance due to adsorption (Ω cm^2)
(CPE)	constant phase element (Ω^{-1} cm^{-2} s^n)
n	constant phase element exponent
$E_{q=0}$	potential of zero charge (pzc)

Greek symbols

β_c	cathodic Tafel slope (mV dec^{-1})
θ	degree of surface coverage
ω	angular frequency (rad s^{-1})
φ	correlative scale of potentials

1. Introduction

Stainless steels are used in various applications such as in the oil and petrochemical industry and as parts of desalination plants [1]. In the latter case, austenitic stainless steels are the most used construction materials due to their good resistance to general corrosion, high strength, workability and weldability. However, their weak point is the susceptibility to localized corrosion in the presence of aggressive ions such as Cl$^-$, which limits their use in seawater. Calcium and magnesium-based deposits in desalination plants are an unavoidable problem. Acids used to remove such scales include HCl, H_2SO_4 and HSO_3NH_2 (sulfamic acid). The application of acid corrosion inhibitors in the treatment of scale parts in multistage flash desalination plants is widely used to prevent or minimize material loss during the contact with acid. In this context, organic compounds containing heteroatoms with high electron density such as nitrogen, sulfur and oxygen or those containing multiple bonds were found to be efficient acid corrosion inhibitors [2,3]. In the oil and petrochemical industry, acetylenic alcohols are particularly effective inhibitors [4]. The simplest member is propargyl alcohol (PA). The nature of PA protective action was subjected to numerous investigations [5–9]. On the other hand, quaternary onium compounds were described as inhibitors against the acid corrosion of iron, steel, zinc, aluminium and Al-alloys [10–13]. The present work aims to investigate the effect of PgTPhPBr towards the corrosion of 304 stainless steel in sulfuric acid solution. This compounds combines the structure of both acetylenic and phosphonium compounds. Previous works indicated that PgTPhPBr is an effective inhibitor for the corrosion of zinc [14] and mild steel [15] in acid solutions. To evaluate the true behaviour of PgTPhPBr, both PrTPhPBr and PA were also studied. Weight loss,

potentiodynamic and electrochemical impedance spectroscopy (EIS) techniques were used.

2. Experimental details

2.1. Preparation of the specimens

The composition of 304 austenitic stainless steel used was: 0.068% C, 0.57% Si, 1.08% Mn, 0.028% P, 8.64% Ni, 18.36% Cr, 0.08% Cu, 0.04% Mo, 0.027% N and Fe remainder. Stainless steel specimens were subjected to heat treatment as described elsewhere [16]. The specimens were mechanically polished using wet emery paper of successive grades, washed thoroughly with bidistilled water, acetone and left for 30 min to obtain reproducible air-formed oxide films [17].

2.2. Weight-loss method

Stainless steel specimens of 15 cm^2 area, in duplicate, were immersed in deaerated 500 cm^3 of 1 M H$_2$SO$_4$ solution without and with various concentrations of the investigated inhibitors for 24 h at 50 °C. The weights of the specimens before and after immersion were determined using an analytical balance XA-200DS (Fischer Scientific). The corrosion rates in mg dm^{-3} day^{-1} (mdd) were calculated and used in calculation of the percentage inhibition efficiency (IE) according to Equation 1:

$$IE = \frac{(CR)_1 - (CR)_2}{(CR)_1} \times 100 \tag{1}$$

where $(CR)_1$ and $(CR)_2$ are the corrosion rate of stainless steel in uninhibited and inhibited H$_2$SO$_4$ solutions, respectively.

2.3. Polarization measurements

Electrochemical experiments were performed in a conventional three electrode thermostated Pyrex glass cell with a graphite rod of large surface area as a counter electrode and a saturated calomel electrode (SCE) as reference. The working electrodes in the form of a plate had a geometric surface area of 0.2 cm^2. Potentiodynamic polarization curves were recorded with the aid of an EG&G PAR potentiostat/galvanostat (model 273) with a corrosion software model 352. Runs were carried out between −150 mV and 2.0 V vs E_{cor} at a scan rate of 1 mV s^{-1}. Solutions were deaerated by bubbling highly pure nitrogen for 2 h before use and continued during the course of measurements. Before recording the polarization curves, the steel electrode was maintained for 30 min, within which a steady state corrosion potential was attained, at open-circuit conditions. Potentiodynamic measurements were conducted in stirred solutions at 50 °C.

2.4. Electrochemical impedance spectroscopy measurements

Electrochemical impedance tests were performed at E_{cor} (a steady state value within 30 min of immersion) with the above-mentioned potentiostat and two-phase EG&G lock-in amplifier (model 5210). The measurements were automatically controlled using an EG&G (M398) software and an IBM PC. Impedance spectra were recorded with a 5 mV sinusoidal perturbation and 5 points per decade at frequencies between 100 kHz and 100 mHz. Frequency points below 100 mHz are highly scattered and have no meaning. The spectra were analysed and interpreted on the basis of the equivalent circuit (EQUIVCRT.PAS) program of Boukamp [18].

3. Results and discussion

3.1. Weight-loss method

Weight-loss measurements of 304 SS in 1 M H$_2$SO$_4$ as a function of concentration of each compound were determined. The corrosion rate of stainless steel in the uninhibited solution was found to be 73 mdd while those obtained in the presence of the investigated compounds are given in Table 1. In the presence of both PgTPhPBr, PrTPhPBr and 1×10^{-5}–1×10^{-4} M PA, the corrosion rate is decreased as the concentration of the additive increased, that is, increase in additive concentration reinforces the inhibition. Inhibition efficiencies attain 98% and 93.4% at 1×10^{-3} M PgTPhPBr and PrTPhPBr, respectively, while complete prevention of SS dissolution is attained at 5×10^{-4} M PA. At 1×10^{-3} M PA, the corrosion rate increased by 40%.

3.2. Potentiodynamic polarization curves

Figures 1, 2 and 3 show the anodic and cathodic polarization curves at 50 °C in 1 M H$_2$SO$_4$ in the absence and presence of 1×10^{-5}–1×10^{-3} M PgTPhPBr, PrTPhPBr and PA, respectively. For the sake of clarity, three of five polarization curves are shown. The electrochemical parameters of corrosion and passivation are given in Table 2. As can be seen from the table, values of E_{cor} are shifted towards more positive potentials with increasing concentration of the compounds except in the presence of 1×10^{-5} and 5×10^{-5} M PA

Table 1. Values of the corrosion rate (mdd) of SS in 1 M H$_2$SO$_4$ in presence of the investigated inhibitors obtained from weight-loss method at 50 °C

[Inhibitor]/M	PgTPhPBr	PrTPhPBr	PA
1×10^{-5}	21.9	27.81	50.37
5×10^{-5}	17.1	20.44	54.02
1×10^{-4}	13.14	12.34	16.79
5×10^{-4}	5.18	10.29	0
1×10^{-3}	1.46	4.82	29.2

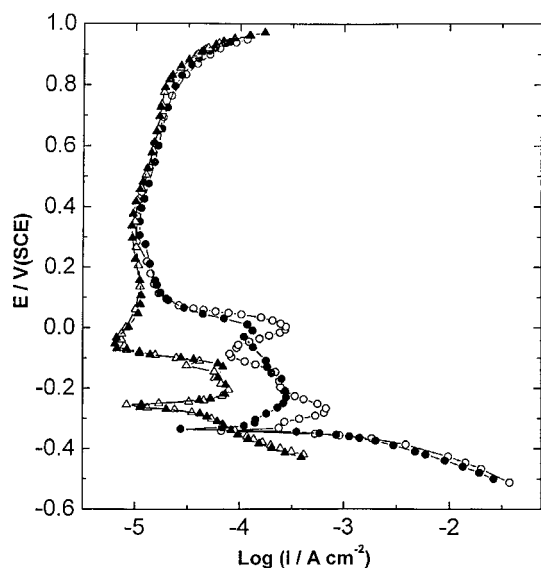*Fig. 1.* Potentiodynamic polarization curves of SS in 1 M H$_2$SO$_4$ with and without PgTPhPBr. Key: (○) pure solution; (●) 5×10^{-5} M PgTPhPBr; (△) 5×10^{-4} M; (▲) 1×10^{-3} M.

Fig. 2. Potentiodynamic polarization curves of SS in 1 M H$_2$SO$_4$ with and without PrTPhPBr. Key: (○) pure solution; (●) 5×10^{-5} M PrTPhPBr; (△) 5×10^{-4} M; (▲) 1×10^{-3} M.
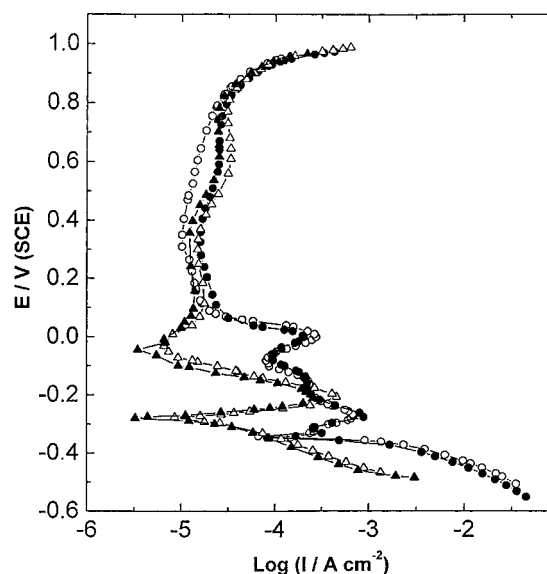
where a slight negative shift is observed. Furthermore, the results indicate that the three compounds (except for PA at concentrations $<1 \times 10^{-4}$ M) reduce the values of I_{cor} (calculated from extrapolation of the linear parts of cathodic Tafel lines to E_{cor}) as the concentration increases. The largest corrosion mitigation is observed at 5×10^{-4} M PgTPhPBr, PrTPhPBr and at 1×10^{-3} M PA. These findings indicate the effectiveness of these compounds as inhibitors for the corrosion of 304 SS in sulfuric acid solution. At concentrations $<1 \times 10^{-4}$ M PA, corrosion acceleration is observed.

Inspection of the polarization curves reveals that the inhibitors shift the cathodic branches to lower current

Fig. 3. Potentiodynamic polarization curves of SS in 1 M H$_2$SO$_4$ with and without PA. Key: (○) pure solution; (●) 5×10^{-5} M PA; (△) 5×10^{-4} M; (▲) 1×10^{-3} M.
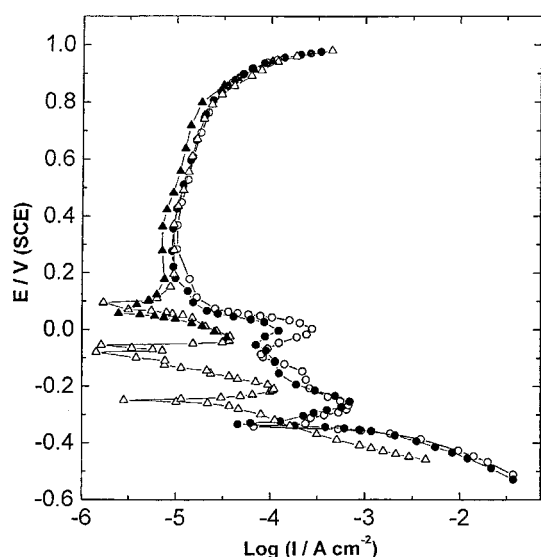
density values without affecting β_c except those obtained in the presence of PgTPhPBr at concentrations $\geqslant 5 \times 10^{-4}$ M, where high values of β_c were obtained. This suggests that the inhibitors are adsorbed on the steel surface without affecting the mechanism of hydrogen evolution (h.e.r.). At 5×10^{-4} and 1×10^{-3} M, PgTPhPBr influences the kinetics of h.e.r. by forming a compact layer on the steel surface. Bockris and Yang [19] observed anomalous values of β_c ($120 \leqslant \beta_c \leqslant 320$ mV decade^{-1}) for h.e.r. in iron corrosion in 0.01 M H$_2$SO$_4$ containing acetylenic alcohol. The influence of PgTPhPBr, PrTPhPBr and PA on the passive behaviour of SS in H$_2$SO$_4$ solution is shown in Figures 1–3, respectively, whereas the passivation parameters are included in Table 2. All the curves indicate an active–passive behaviour. Both the phosphonium compounds shift the E_{pp} to more positive values and the shift is more pronounced in the case of PgTPhPBr. For the acetylenic compound, PA, the positive shift in E_{pp} occurs only at concentration $\geqslant 1 \times 10^{-4}$ M. The value of I_{a1} obtained in the pure medium was found to decrease in the presence of 1×10^{-5}–1×10^{-3} M PgTPhPBr and to attain a value of 100 μA cm^{-2} at 1×10^{-3} M. PrTPhPBr and PA increase the value of I_{a1} at lower concentrations but both compounds reduce I_{a1} at higher concentrations ($\geqslant 1 \times 10^{-4}$ M PrTPhPBr and $\geqslant 5 \times 10^{-4}$ M PA). A spontaneous passivation occurs for SS in the presence of 1×10^{-3} M PrTPhPBr. It is clearly observed from Figures 1–3 that the passive range obtained in the pure acid solution becomes broader for PgTPhPBr. Based on the remarkable decrease in I_{a1} and the wide passive range, PgTPhPBr can be considered as a good organic passivator for SS in sulfuric acid at 50 °C. Inspection of Figures 1–3 reveals a characteristic feature in the passive zone, that is, the appearance of a second anodic current peak around 0 V vs SCE at concentrations $\leqslant 5 \times 10^{-4}$ M after which these

Table 2. Corrosion and passivation parameters for SS in 1 M H_2SO_4 with and without inhibitors at 50 °C

[Inhibitor] /M	$-E_{cor}$ /mV	I_{cor} /μA cm^{-2}	β_c /mV dec^{-1}	$-E_{pp}$ /mV	I_{a1} /μA cm^{-2}	I_{a2} /μA cm^{-2}
0.0	340	1657	113	272	692	278
PgTPhPBr						
1×10^{-5}	336	1089	108	242	490	173
5×10^{-5}	335	1000	108	180	302	138
1×10^{-4}	305	279	95	173	275	107
5×10^{-4}	258	32	181	125	79	–
1×10^{-3}	256	33	213	129	80	–
PrTPhPBr						
1×10^{-5}	338	1535	119	264	758	178
5×10^{-5}	332	1501	112	259	721	123
1×10^{-4}	330	604	105	252	547	40
5×10^{-4}	248	28	118	209	110	38
1×10^{-3}	170	–	–	–	–	–
PA						
1×10^{-5}	352	1999	130	282	977	274
5×10^{-5}	347	1660	129	272	955	207
1×10^{-4}	320	489	103	270	708	170
5×10^{-4}	282	252	107	207	456	–
1×10^{-3}	280	22	121	215	264	–

peaks are no longer present. Values of I_{a2} are included in Table 2. The magnitude of I_{a2} obtained in the pure medium decreased in the presence of the inhibitors.

The appearance of the second anodic peak in the polarization curve of SS in sulfuric acid was observed previously [20–23]. The second anodic current peak was attributed to reoxidation of adsorbed H atoms on the SS surface. Phosphorous, as a minor element (~0.03% in SS under study), accumulates at the corroded steel surface and poisons the hydrogen evolution reaction. It inhibits H—H recombination and consequently increases the amount of adsorbed hydrogen on the steel surface [21, 24]. In this study, the investigated inhibitors reduced the magnitude of I_{a2} by about 39–86% at concentrations $\leqslant 1 \times 10^{-4}$ M. The peak completely disappeared at higher concentrations. This is due to one or both of the following actions:

(i) The adsorbed inhibitor decreases the dissolution of SS and consequently decreases accumulation of the poisoning phosphorous on the electrode surface.
(ii) The adsorption of the inhibitor decreases the surface area available for adsorbed hydrogen. This can be confirmed by comparing the values of I_{cor} and I_{a2} for both PrTPhPBr and PA at concentrations of 5×10^{-5} and 1×10^{-4} M. The decrease in accumulation of P on the steel surface is not the unique reason for the decrease of I_{a2}. The large phosphonium molecule occupies a larger surface area than the smaller PA [19], so that the decrease in I_{a2} is more pronounced for phosphonium compounds than for PA.

3.3. *Impedance measurements*

Impedance measurements on the SS in 1 M H_2SO_4 solutions alone and in the presence of various concentrations (1×10^{-5}–1×10^{-3} M) of PgTPhPBr, PrTPhPBr and PA were performed at open-circuit corrosion potential. Figure 4 shows the influence of PgTPhPBr on the impedance spectra of SS in the form of a Nyquist plot. The spectra recorded for the pure acid solution and in the presence of concentrations $\leqslant 1 \times 10^{-4}$ M of all additives display two capacitive loops (Figure 4(a)). The high-frequency (h.f.) loop is located between 1 Hz and 10 kHz and can be attributed to the charge transfer process while that observed in the low-frequency (l.f.) region is located below 1 Hz and can be attributed to the adsorption of hydrogen or adsorption of the inhibitor molecules on the SS surface in the pure acid solution without and with the inhibitor, respectively. Armstrong et al. [25] indicated that when charge transfer is important (either at high frequency or when diffusion is unimportant) and when the electroactive species are always at their Nernstian concentration at the electrode surface, the complex plane impedance exhibits a single semicircle, but in the presence of more complex phenomena (adsorption, desorption), the complex plane impedance includes supplementary loops. These loops are either capacitive or inductive depending on the mode of action of the adsorbates in the electrochemical reaction. Although the h.f. loops have semicircular appearance, they are depressed. Deviations of this kind, often referred to as frequency dispersion, have been attributed to nonhomogeneity of the solid surface [26]. A practical way to represent distributed processes such as corrosion of rough and nonhomogenous electrode is the use of the constant phase element (*CPE*) for which the impedance given by

$$Z_{CPE} = [Y_o(j\omega)^n]^{-1} \qquad (2)$$

where Y_o is a general admittance function, j is the complex operator $\sqrt{(-1)}$, ω is the angular frequency of a.c. excitation and n is an empirical exponent [27]. When
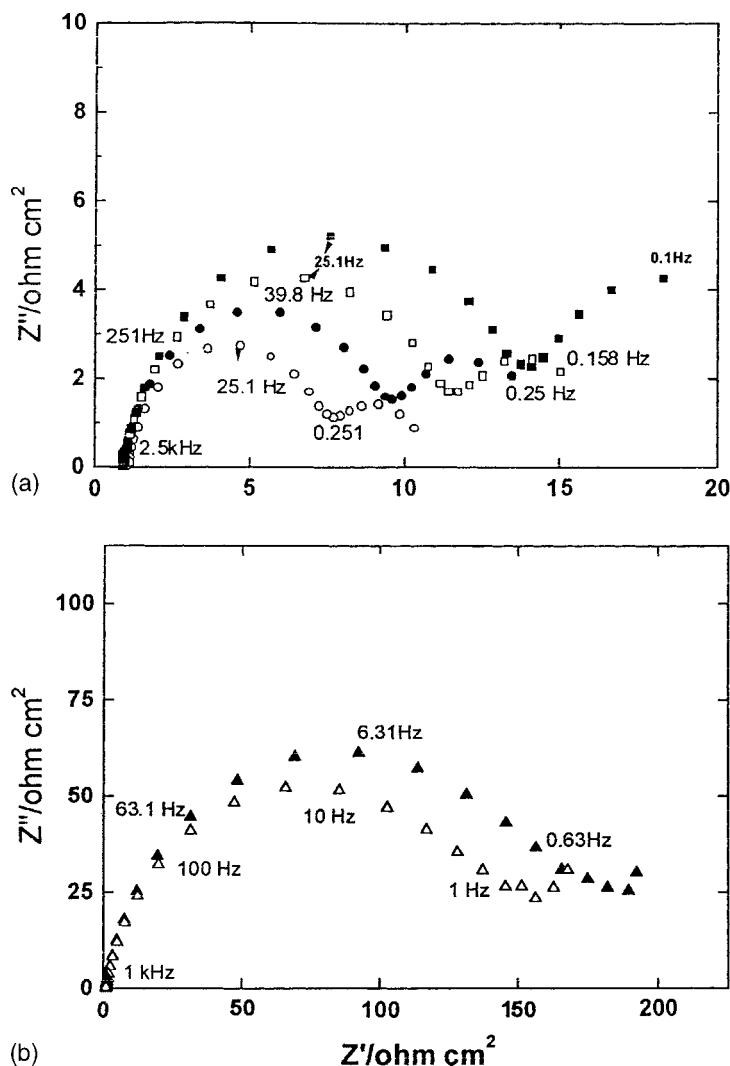
Fig. 4. Nyquist plots obtained at E_{cor} for SS in 1 M H_2SO_4 with and without PgTPhPBr at different concentrations. For A: ($\bigcirc$) 1 M H_2SO_4; ($\bullet$) 1×10^{-5} M PgTPhPBr; ($\square$) 5×10^{-5} M; ($\blacksquare$) 1×10^{-4} M. For B: ($\blacktriangle$) 5×10^{-4} M PgTPhBr; ($\triangle$) 1×10^{-3} M.

$n = 0$, there is no imaginary component, and the impedance is represented by a real resistance R. If $n = 1$, the impedance is best described by a capacitor, so that $Y_o = C$. For the case of $n = 0.5$, an impedance relation, known as the Warburg impedance, is applicable; this impedance is associated with concentration and diffusion related processes [28].

However, Figure 5(a) represents the equivalent circuit used to fit the experimental data of Figure 4(a). This consists of two circuits in series, the first contains $(CPE)_1$ (constant phase element related to the double layer capacity) in parallel to R_{ct} (resistance of charge transfer) due to the corrosion process while the second circuit contains $(CPE)_2$ and R_a due to the adsorption. On the other hand, the equivalent circuit displayed in Figure 5(b) was employed for modeling the impedance spectra of Figure 4(b) where only one capacitive loop is observed. To ensure the validity of the proposed equivalent circuits and the estimated impedance parameters, the impedance results were subjected to nonlinear least square fit within the limits of experimental errors and reproducibility of data. Comparison between the experimental and simulated results obtained, for example, in presence of 1×10^{-5} M PgTPhPBr, is shown in Figure 6 and clearly indicate that the proposed equivalent circuits are the most probable ones. For the three compounds, values of R_{ct} and $(CPE)_1$ were estimated and those of R_{ct} were plotted as a function of the additive concentrations (Figure 7). As the concentrations of the additives increase, the value of R_{ct} obtained in the pure medium (6.75 Ω cm^2) increases regularly up to 1×10^{-4} M and then jumps to a maximum value (166 and 240 Ω cm^2) at 1×10^{-3} M PgTPhPBr and PrTPhPBr, respectively, and (161 Ω cm^2) at 5×10^{-4} M PA. The curve obtained for PgTPhPBr lies between those obtained for PrTPhPBr and PA. On the other hand, the value of $(CPE)_1$ obtained in the pure acid solutions $((CPE)_1 = 1.68 \times 10^{-3}$ Ω^{-1} cm^{-2} $s^n)$ was found to decrease gradually up to 1×10^{-4} M $((CPE)_1 = 1.14 \times 10^{-3}$–$1.5 \times 10^{-4}$ Ω^{-1} cm^{-2} $s^n)$ after which a large drop $((CPE)_1 = 2.3 \times 10^{-4}$–$4.4 \times 10^{-4}$ Ω^{-1} cm^{-2} $s^n)$ was observed. The value of the constant phase element exponent, n, remains approximately the same in the uninhibited and inhibited solutions. The increase in R_{ct}
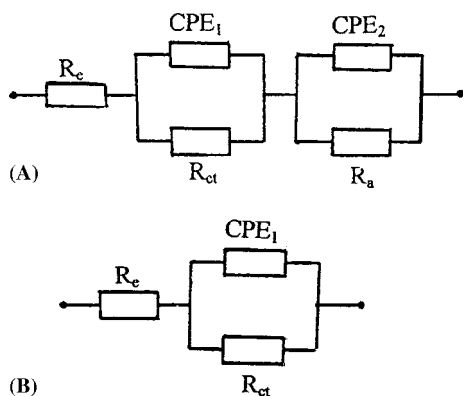
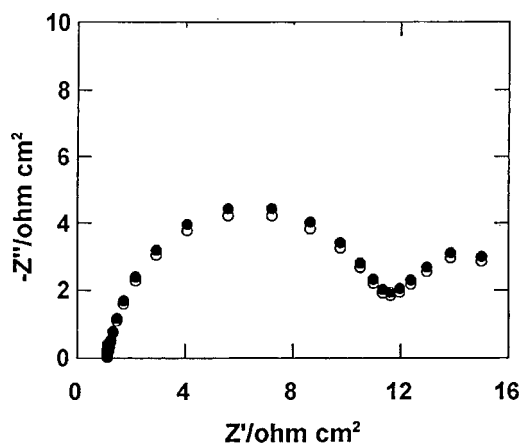Fig. 5. Equivalent circuits (A and B) used for modelling the impedance results.

Fig. 7. Variation of R_{ct} values with the concentrations of the inhibitors. Key: (○) PgTPhBr; (●) PrTPhPBr; (△) PA.

Fig. 6. Comparison of the experimental (○) and simulated (●) impedance data obtained for the corrosion of SS in 1 M H$_2$SO$_4$ containing 1×10^{-5} M PgTPhPBr.

values indicates the increase in corrosion resistance of SS whereas the decrease in $(CPE)_1$ values can be attributed to the decrease in the surface area of the electrode surface exposed to the corrosive medium (increase in the area covered by the inhibitor). The value of n can be used as an indicator for the corrosion mechanism. The approximate constancy of n reveals that the charge transfer process controls the corrosion mechanism of SS in H$_2$SO$_4$ without and with the inhibitors.

At high inhibitor concentrations, $\geqslant 5 \times 10^{-4}$ M, the l.f. capacitive loop disappeared. This can be attributed to the complete coverage of the electrode surface by the inhibitor molecules. In such cases the appearance of a small capacitive loop at h.f. values is expected. In the present study, such an h.f. loop was not detected. However, many inhibited corrosion systems [29–33] did not show either the l.f. capacitive loop relevant to the adsorption process nor the expected h.f. loop due to the formation of an inhibitor layer.

Based on the same mechanism of corrosion, values of R_{ct} (which are inversely proportional to the corrosion
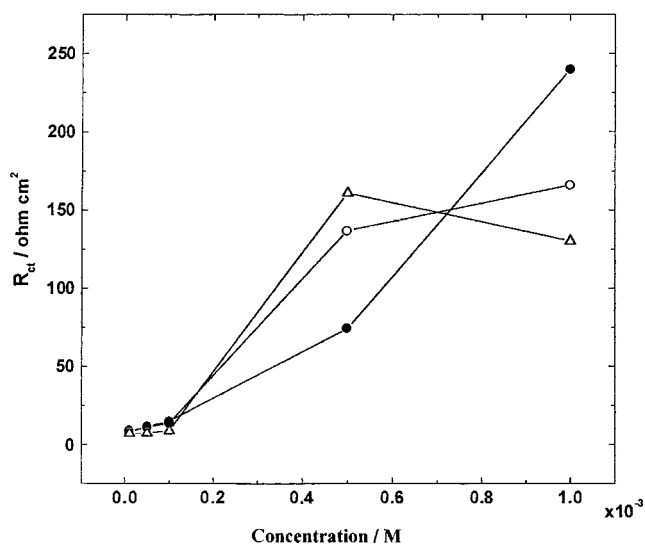
rate) can be used for calculating the percentage inhibition efficiency according to

$$IE = \frac{R_{ct} - R_{ct}^o}{R_{ct}} \times 100 \tag{3}$$

where R_{ct}^o and R_{ct} are values of charge transfer resistance in sulfuric acid without and with the inhibitors, respectively. Values of percentage IE calculated from Equation 3 and those obtained from potentiodynamic polarization techniques are given in Table 3. Except at concentrations $\leqslant 5 \times 10^{-5}$ M PrTPhPBr and PA, there is a reasonable agreement between values of IE% calculated from the two methods.

3.4. Adsorption isotherms

The degree of surface coverage (θ) can be calculated from the following:

$$\theta = 1 - \frac{I_{inh}}{I_{uninh}} \tag{4}$$

For the investigated inhibitors, a correlation was found between the degree of surface coverage calculated from the impedance measurements and log C. The experimental results obtained for PgTPhPBr, PrTPhPBr and PA have been applied to many adsorption isotherms. Adsorption of both PgTPhPBr and PA follow the Frumkin isotherm (θ against log C is a S-shaped curve) while adsorption of PrTPhPBr obeys that of Temkin, θ is a linear function of log C, (Figure 8). At concentrations of 5×10^{-5}–5×10^{-4} M, the adsorption behaviour of PgTPhPBr is similar to that of PrTPhPBr (θ vs log C is a straight line). So, PgTPhPBr combines the adsorption behaviour of the onium and acetylenic compounds.

Table 3. Values of the percentage inhibition efficiency (*IE*) obtained from cathodic polarization and EIS techniques

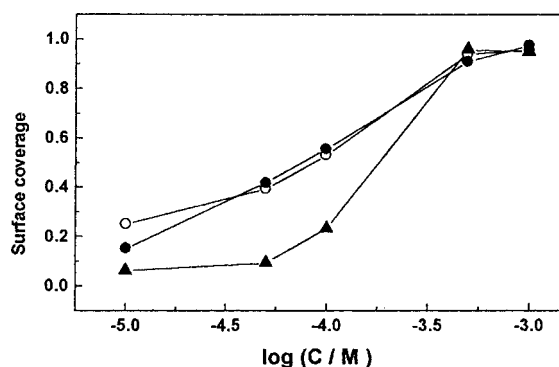| [Inhibitor] /M	PgTPhPBr		PrTPhPBr		PA	
	Tafel	R_{ct}	Tafel	R_{ct}	Tafel	R_{ct}
1×10^{-5}	34.3	25.0	7.0	15	−21.0	6.3
5×10^{-5}	40.0	39.3	9.5	42.0	0.0	9.4
1×10^{-4}	83.0	53.0	63.5	55.7	70.5	23.3
5×10^{-4}	98.0	94.0	89.3	91.0	85.0	95.8
1×10^{-3}	98.0	95.5	98.0	97.4	98.7	94.8

Fig. 8. Adsorption isotherms of PgTPhPBr, PrTPhPBr and PA on SS surface. Key: (○) PgTPhBr; (●) PrTPhPBr; (▲) PA.

3.5. *Mechanism of corrosion inhibition or acceleration*

The present study attributes inhibition of stainless steel corrosion in H_2SO_4 to the adsorption of PgTPhPBr, PrTPhPBr and PA on the steel surface. The adsorption process depends on the charge of the electrode surface that can be determined according to the correlative scale (φ-scale) of potentials [34]:

$$\varphi = E_{cor} - E_{q=0} \tag{5}$$

where $E_{q=0}$ is the potential of zero charge (pzc). According to Brigham [35], the pzc of 18-8 stainless steel in acidic sulfate solution at 50 °C is about −450 mV vs SCE. Accordingly, the ϕ potential of the stainless steel is +110 mV and the steel surface is positively charged at the corrosion potential. Hence, adsorption of cationic species, like $PgTPhP^+$ and $PrTPhP^+$, is not favorable while negatively charged species, like Br^- ions, are preferentially adsorbed at the steel surface. The adsorption of Br^- ions gives the surface a negative charge at E_{cor} and in turn favors electrostatic adsorption of onium cation, and a positive synergistic effect arises. In addition, the adsorbed cations can be oriented with the ring structure parallel to the steel surface and adsorption via interaction of π-electron of the benzene ring is possible. Such electronic interaction increases by participation of the carbon–carbon triple bond of the propargyl group in case of PgTPhPBr. Ayer and Hackerman [36] reported that π-electron interaction is stronger than electrostatic or charge transfer interaction.

The accelerating effect or the poor inhibition exerted by PA at lower concentrations ($\leqslant 5 \times 10^{-5}$ M) can be ascribed to the electrochemical reduction of PA to allyl alcohol at E_{cor} [37]. At high concentrations, PA acts as an efficient inhibitor due to adsorption of the compound at the steel surface through the π-electron interaction of the triple bond and the steel surface (the triple bond is the focal point of the inhibitive effect of the acetylenic compounds in acid solutions). On the other hand, desorption of PA molecules from the electrode surface may account for the acceleration of the anodic dissolution of SS. Desorption of PA near the corrosion potential was reported by Aksut [37] and Hackerman [5].

4. Conclusions

In deaerated 1 M H_2SO_4 at 50 °C, PgTPhPBr inhibits effectively the corrosion of SS and acts as a good passivator by forming a compact layer on the steel surface. In comparison with PrTPhPBr and PA, PgTPhPBr was found to combine the behaviour of both phosphonium and acetylenic compounds. Depending on the measurement of I_{a2}, the investigated compounds decrease the adsorption of hydrogen on the stainless steel surface. EIS measurements indicate that the charge transfer process controls the corrosion mechanism of SS in H_2SO_4 without and with the inhibitors.

References

1. 'Stainless Steel Europe' Wiley Van der Hoven *Chem. Eng.* **6** (9) (1994), p. 49.
2. I.L. Rozenfeld, 'Corrosion Inhibitors' (McGraw-Hill, New York, 1981).
3. A.M. Al-Mayouf, A.A. Al-Suhybani and A.K. Al-Ameery, *Desalination* **116** (1998) 25 and references therein.
4. G.L. Foster, B.D. Oakes and C.H. Kucera, *Ind. Eng. Chem.* **51** (1959) 825.
5. M. Bartos and N. Hackerman, *J. Electrochem. Soc.* **139** (1992) 3428.
6. D. Jayaperumal, S. Muralidharan, P. Subramanian, G. Venkatachari and S. Senthilvel, *Anti-Corros. Meth. Mater.* **44** (1997) 265.
7. M.S. Morad, *Mater. Chem. Phys.* **60** (1999) 188.
8. Y. Feng, K.S. Siow, W.K. Teo and A.K. Hsieh, *Corros. Sci.* **41** (1999) 829.
9. M. Gojic, *Corros. Sci.* **43** (2001) 919.
10. W.J. Lorenz and H. Fischer, *Ber. Bunsenges Phys. Chem.* **69** (1965) 689.
11. M. Morad, J. Morvan and J. Pagetti, 8th European Symposium on 'Corrosion Inhibition', Ann. Uni. Ferrara, N.S. Sez., Suppl. **10** (1995) 159.
12. M.S. Abdel Aal and M.S. Morad, *Br. Corros. J.* **36** (2001) 253.
13. M.S. Abdel-Aal, M.Th. Makhlof and A.A. Hermas, 7th European Symposium on 'Corrosion Inhibition', Ann. Uni. Ferrara, N. S. Sez., Suppl. **9** (1990) 1143.
14. M.S. Morad, *J. Appl. Electrochem.* **29** (1999) 619.
15. M.S. Morad, *Corros. Sci.* **42** (2000) 1307.
16. A.A. Hermas, K. Ogura, S. Takagi and T. Adachi, *Corrosion* **51** (1995) 3.

102

17. P. Chen, T. Shinohara and S. Tsujikawa, Proceedings of the 41th Japan Corrosion Conference, JSCE, Oct., Matsuyama, Japan (1994), p. 85.
18. B.A. Boukamp, 'Equivalent Circuit (EQUIVCRT. PAS), User's Manual' (2nd edn., 1989).
19. J.O'M. Bockris and B. Yang, *J. Electrochem. Soc.* **138** (1991) 2237.
20. A.A. Hermas, K. Ogura and T. Adachi, *Electrochim. Acta* **40** (1995) 837.
21. A.A. Hermas and K. Ogura, *Electrochem. Acta* **41** (1996) 1601.
22. A.A. Hermas, M.S. Morad and K. Ogura, *Corros. Sci.* **41** (1999) 2251.
23. A.A. Hermas, *Br. Corros. J.* **34** (1999) 132.
24. G. Zheng, B. Popov and R.E. White, *J. Electrochem. Soc.* **141** (1994) 1526.
25. R.D. Armstrong, M.F. Bell and A.A. Metcalf, 'Specialist Periodical Reports of Electrochemistry', Vol. **6** (Chemical Society, London, 1978), p. 98.
26. K. Juttner, *Electrochim. Acta* **35** (1990) 1501.
27. F.B. Growcock, *Chem. Technol.* **19** (1989) 564.
28. K. Hladky, L.M. Callow and J.L. Dawson, *Br. Corros. J.* **15** (1980) 20.
29. E. McCafferty and J.V. McArdle, *J. Electrochem. Soc.* **142** (1995) 1447.
30. S. Muralidharan, K.L. Phani, S. Pitchumani, S. Ravichandran and S.V.K. Iyer, *J. Electrochem. Soc* **142** (1995) 1478.
31. E. Guilminot, J-J. Rameau, F. Dalard, C. Degrigny and X. Hiron, *J. Appl. Electrochem.* **30** (2000) 21.
32. M.A. Quraishi, J. Rawat and M. Ajmal, *J. Appl. Electrochem.* **30** (2000) 745.
33. A. Popova, E. Sokolova, S. Raicheva and M. Christov, *Corros. Sci.* **45** (2003) 33.
34. L.I. Antropov, *J. Phys. Chem. USSR* **25** (1951) 1494; 37 (1963) 865.
35. R.T. Brigham, *Corros. Sci.* **29** (1989) 995.
36. R.C. Ayer and N. Hackerman, *J.Electrochem. Soc.* **110** (1963) 21.
37. A.A. Aksut, *Electrochim. Acta* **28** (1983) 1177.